Preferential nucleation and high mobility of linear Cu trimers on Ag(111)

A. W. Signor and J. H. Weaver*

Department of Materials Science and Engineering, University of Illinois at Urbana-Champaign, Urbana, Illinois 61801, USA

(Received 12 August 2010; revised manuscript received 13 February 2011; published 24 October 2011)

Using scanning tunneling microscopy, we studied the formation of dimers, trimers, and other clusters of Cu on Ag(111) at low temperature. We show that trimers, once formed, have significantly higher mobilities than either atoms or dimers. While transient, this mobility makes linear trimers a major contributor to mass transport. Using the scanning tunneling microscopy tip, we constructed linear and compact trimers at 5 K and investigated their stabilities and diffusion parameters as a function of temperature. Analysis shows that the diffusion barrier for linear trimers is very low, 13.6 meV, compared to 65 meV for atoms, while the compact trimer is stable and immobile. Thus, significant diffusion of this nonequilibrium cluster can occur before the equilibrium compact trimer is reached. The details of trimer diffusion and rotation provide insights into the intermediate diffusion steps and indicate that the large lattice mismatch plays an important role. The properties of Cu trimers on Ag(111) contrast with those reported for homoepitaxial trimers on fcc(111) surfaces. Because the diffusion phenomena for Cu trimers and other clusters on Ag(111) are largely a result of lattice mismatch, similar phenomena may exist in the early stages of nucleation and growth of other heteroepitaxial systems.

DOI: 10.1103/PhysRevB.84.165441 PACS number(s): 68.35.Fx, 68.35.bd, 68.35.Gy, 68.37.Ef

I. INTRODUCTION

Surface diffusion of atoms and clusters has been studied for decades, driven in large part by the importance of the processes leading to mass transport on surfaces. This work has revealed a diversity of surface diffusion phenomena, especially for cluster diffusion because of the numerous ways a collection of atoms can move on a surface.[1–4] The mobility of small clusters can have significant implications on the nucleation density and island size distribution in the early stages of growth,[5–9] and the diffusion of large islands leads to coarsening in the late stages.[10–18]

Despite their importance, relatively little direct, quantitative experimental work has been done regarding the stability and diffusion of small clusters. Because the majority of cluster diffusion studies have focused on homoepitaxial systems, even less is known about the role of lattice mismatch in determining the properties of heteroepitaxial clusters despite predictions of interesting phenomena.[19,20] While the mobility of larger islands generally decreases with size, several cases of nonmonotonic size dependencies[21–32] and, remarkably, cases where clusters have even higher mobility than individual atoms, have been reported.[27–32]

In this paper, we focus on Cu trimers on Ag(111) and demonstrate that, depending on their structure, they can have significantly more mobility than either atoms or dimers. Using low-temperature scanning tunneling microscopy (STM), we have previously shown that larger clusters have surprisingly low diffusion barriers and a novel dislocation mechanism that is related to the ∼12% lattice mismatch for Cu on Ag(111).[25,26] Here, we show that Cu trimers diffuse large distances following their formation. Studies at 24 K show that this trimer mobility is transient, and the mobile trimers are equilibrated in a compact, immobile state or coalesce with other particles. To determine the structure of the mobile precursor, we used the STM tip to construct both compact and linear chain trimers at 5 K. The linear chain trimers underwent lengthwise hopping along the close-packed ⟨110⟩ directions and rotated about an end atom at $T \geqslant 8$ K while maintaining a linear shape. The hop and rotation rates were measured between 8–12 K, yielding a diffusion barrier of 13.6 meV, only ∼1/5 the diffusion barrier of individual atoms, 65 meV. In contrast, the compact trimer constructed at 5 K was immobile. We conclude that the large displacements upon trimer formation are due to a precursor, namely the linear trimer. The linear trimer has a very low diffusion barrier, and it is a very important contributor to mass transport for Cu on Ag(111). The broader and more surprising implication of this work is that significant diffusion of a nonequilibrium cluster can occur before the equilibrium structure is reached. Furthermore, while previous reports of transient mobility have been related to the enthalpy released upon condensation, our results point to a case of transient mobility results from a nonequilibrium structure, which is favored upon cluster nucleation.

II. SAMPLE PREPARATION AND ATOM MANIPULATION

Experimental measurements were carried out in an Omicron low-temperature scanning tunneling microscope that operates at 4.5–300 K. The sample stage was enclosed by a cryogenically cooled metal shroud, which helped regulate the temperature and keep the surface clean for the long times required for the diffusion measurements. The Ag(111) substrates were thick films (100's of monolayers) grown in a preparation chamber (base pressure $\sim 4 \times 10^{-11}$ Torr) by evaporating Ag onto Si(111)-7 × 7 at ∼20 K, followed by an anneal at ∼600 K for a few seconds. These films have large, flat regions free of defects or steps,[33] making them ideal for diffusion studies. The excellent agreement between our measurements of Cu atom and dimer diffusion barriers with those measured on Ag(111) single crystals[34] indicate a high-quality surface. This also provides a confirmation of temperature accuracy.

Once the substrate was prepared, the sample was moved to the STM stage and cooled to ∼5 K. A homebuilt evaporator attached to the measurement chamber enabled deposition of dilute amounts of Cu while the sample was on the STM stage at 5 K. The Cu source was heated in a W basket, and the exterior

of the evaporator was water cooled to minimize outgasing. During evaporation, the pressure remained below 10^{-10} Torr. A small aperture created a narrow beam, protecting the critical components of the microscope and limiting exposure to the sample surface. A quartz crystal microbalance mounted in the evaporator was used to monitor the flux, and it was calibrated by counting individual atoms in STM images collected at 5 K immediately after exposure. This, combined with a shutter, allowed for precise control of the amount of Cu, and it enabled the early stages of nucleation and growth to be observed *in situ* as the sample was warmed from 5 K.

To construct compact and linear trimers at 5 K, the tip was positioned above the atom to be moved, and the tunneling parameters were changed to bring it close enough to allow an attractive interaction. The tip was then moved at $\sim$1 nm s^{-1} to the desired location, pulling the atom along with it. To release the atom, the tunneling parameters were reset to those used for imaging (0.5 V, 0.3 nA). To establish the optimal tunneling conditions, manipulation attempts were repeated while the tunneling current was gradually increased, bringing the tip incrementally closer to the surface, until a successful manipulation was achieved. The optimal parameters for manipulation were 0.5 V and 6.0 $\pm$ 1 nA, though the parameters and success rate varied depending on the condition of the tip. This procedure was adapted from those used in other studies of fcc(111) metals surfaces.[35,36]

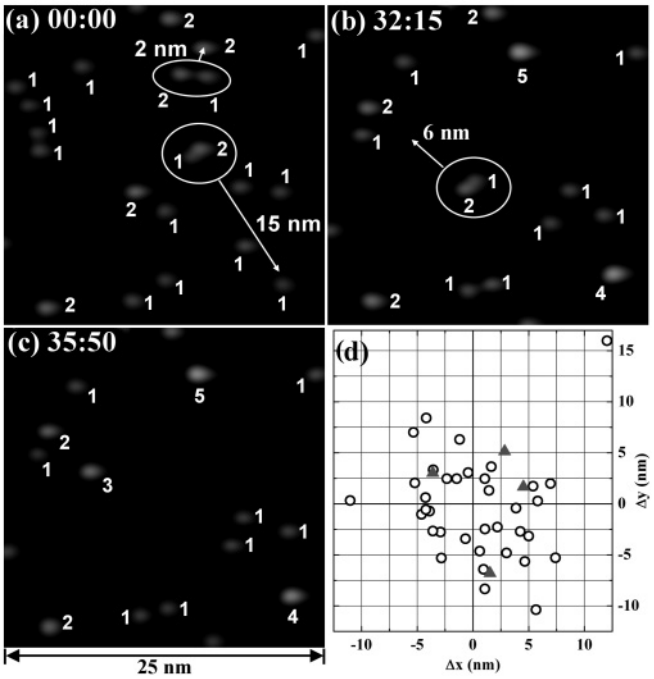

FIG. 1. (a)–(c) diffusion of Cu atoms, dimers, and trimers on Ag(111) at 24 K. The labels indicate particle size, the ellipses particles prior to coalescence, and arrows the relocation of trimers upon their formation. (d) Displacement vectors referenced to the center of mass of the atom-dimer pairs immediately prior to coalescence. The black circles represent trimers that coalesced with other particles, the red triangles trimers that were spontaneously immobilized. As discussed in the text, trimer formation produced mobile linear chains and conversion of those chains to compact structures immobilized them.

III. TRIMER NUCLEATION AND RAPID DIFFUSION

Figure 1 presents a series of images collected at 24 K that show trimer nucleation and subsequent rapid displacement. The labels indicate the number of atoms in each particle, a number that is known precisely because cluster formation events were observed directly, starting from individual atoms. Note that the elongated shape of particles in Fig. 1 is not real, but rather an artifact of the fast scanning speed and the finite response time of the feedback loop. For the atoms and dimers, diffusion barriers match previously published values.[34] The images in Fig. 1 were selected from a set of $\sim$150 with $\sim$215 s between frames ($\sim$9 h of imaging). In (a), the ellipses highlight atom-dimer pairs in close proximity, prior to their combination. During the time between frames, the resulting trimers moved 2 or 15 nm to the positions indicated and coalesced with a dimer or atom to form the pentamer and tetramer shown in (b). Note that image (b) of 32 min was selected to show the small and slower displacements of the atoms and dimers in the viewing area. The highlighted atom-dimer pair in (b) had combined in the next image (c) and had moved 6 nm before being immobilized without coalescence. This trimer and all others that were immobilized had compact shapes, and they were stable during the measurement time of several days at 20–24 K.

Figure 1(d) summarizes the displacements for 39 trimer formation events. The points represent the coordinates of the final location referenced to the center of mass of the atom-dimer pair immediately prior to coalescence. The (red) triangles represent four trimers that were immobilized on the pristine surface, as in (c), and the black circles represent those that ultimately coalesced with other ad-particles, as in (b). The displacements ranged from 2–20 nm, and all occurred within the time between images (80–215 s). Since the atom and dimer positions were continuously monitored, we can conclude that all trimer formation events resulted in rapid diffusion.

From Fig. 1, it is clear that trimer nucleation results in a cluster that has significantly more mobility than atoms or dimers. The fact that several trimers were immobilized on the surface without encountering other ad-species demonstrates that their intrinsic mobility is short lived. While it is possible that they were trapped at undetectable defects on the surface, one would expect atoms and dimers to be trapped as well, yet they all maintained the expected diffusivity. Furthermore, in one instance, a diffusing atom probed the future resting site of a trimer without any change in its diffusion properties, strengthening the case that the trimers are immobilized on a pristine surface, that the mobility is naturally transient, and that there is something special about the trimer formation event that leads to a very mobile species that ultimately converts to the immobile trimer.

Based on the data of Fig. 1(d), the mean-squared displacement is 44.6 nm^2. Assuming two-dimensional diffusion, we can deduce a lower limit on the diffusivity of the mobile precursor using the Einstein relation, $D \geqslant \langle \Delta r^2 \rangle / 4\tau$, where $\langle \Delta r^2 \rangle$ is the mean-squared displacement and τ is the time between images. It is important to note that this estimation provides only a lower limit on the diffusivity since, with the experimental time resolution, we only observe initial and final locations. Based on this analysis, the lower limit on

the diffusivity is $\sim 5 \times 10^{-16}$ cm^{2}s^{-1}, compared to $\sim 4 \times 10^{-18}$ cm^{2}s^{-1} for atoms. Assuming the normal prefactor of 10^{-3} cm^{2}s^{-1}, this establishes an upper limit on the diffusion barrier of ~58 meV compared to 65 meV for individual atoms, though it is possibly much lower than that. This low barrier is surprising in light of molecular dynamics simulations that predict a barrier of ~290 meV, prohibitively large to allow diffusion at 24 K.[25,26,37] In these simulations, the ground state of a Cu trimer on Ag(111) was a compact triangle with all atoms in fcc sites, and diffusion occurred in a concerted fashion. In agreement with the simulations, compact trimers were immobile at 24 K. While the above has considered thermal diffusion, there is the possibility that a contribution to displacement might arise from the energy associated with bond formation upon dimer and atom binding. This is unlikely since nucleation of dimers and larger particles never resulted in movement, and we conclude that the contribution from the formation enthalpy is small and cannot account for the large displacements observed for Cu trimers.

IV. MOBILE LINEAR AND IMMOBILE COMPACT TRIMERS

From the data of Fig. 1, one cannot conclude much regarding the nature of the precursor; only the initial and final locations are known. Given the predicted and experimentally observed stability of compact trimers, we reasoned that the mobile precursor has a different structure. To learn more about the structure of the mobile trimer presented considerable experimental challenges. At temperatures where trimers form on the experimental time scale, their mobility is too high and too short lived to allow structural investigations. Accordingly, we reduced the temperature and used the STM tip to manipulate individual atoms, as outlined above, to construct linear and compact trimers. Figure 2 shows the construction of a linear trimer at 5 K. Three Cu monomers are indicated in (a). The atom on the left was brought into contact with the middle atom in (b). The orientation of the dimer was established, and the third atom was moved to the end of the dimer in (c), forming a linear trimer oriented along the close-packed [0$\bar{1}$1] direction. The linear trimer was stable and immobile at 5 K.

To investigate the properties of linear trimers, we increased the temperature while continuously imaging. Significantly, the temperature at which trimer motion was first observed was 8 K, extremely low compared to the 19 K onset for adatom motion.

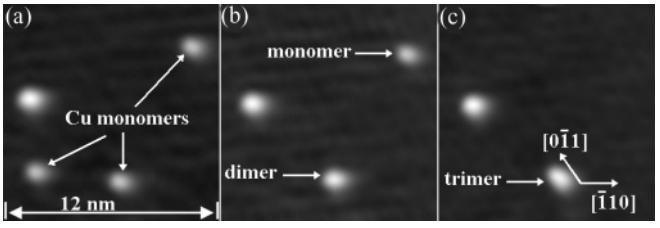

FIG. 2. Assembly of a linear-chain trimer using the STM tip at 5 K. The atom on the left in (a) was brought into contact with the middle atom, forming the dimer in (b). In (c), the third atom was moved to form a linear trimer chain oriented along [0$\bar{1}$1]. The trimer chain was stable and immobile at 5 K; imaging parameters 0.5 V, 0.3 nA; manipulation parameters 0.5 V, 6.0 nA.

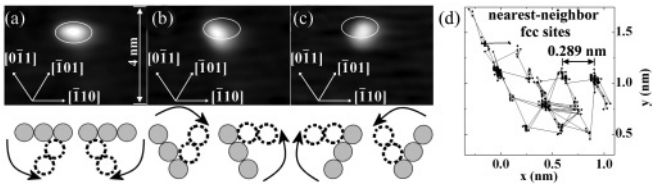

FIG. 3. Rotation and diffusion of linear trimers at 8.5 K. The trimer orientation is (a) [$\bar{1}$10], (b) [0$\bar{1}$1], and (c) [$\bar{1}$01]. Hopping along the long axis and rotation about an end atom occur with equal probability; rotation around the center atom never occurs. Both lengthwise hopping and rotation result in a displacement of the center of mass by one Ag(111) nearest neighbor distance, 0.289 nm, shown in the representative trajectory in (d). The rotation direction depends on chain orientation and pivot atom, with the only observed rotations depicted in the models below the images. The solid circles indicate the initial atom locations, the open circles the final locations, and the arrows the directions of rotation.

Two types of motion occurred with equal probability in the 8–9 K range, namely lengthwise hopping along close-packed ⟨110⟩ directions and rotation about an end atom. Although rotations about each end had equal probability, rotation about the middle atom was never observed. The images in Fig. 3 obtained at 8.5 K show the changes in orientation associated with rotation. The chain is oriented along [$\bar{1}$10] in (a), [0$\bar{1}$1] in (b), and [$\bar{1}$01] in (c). The ellipses help distinguish the different orientations. A particle tracking program[38] was used to extract the trimer trajectory, and nearby immobile atoms were used as a reference to correct for drift of the microscope. Figure 3(d) is a representative trajectory of one of the linear trimers, comprised of a discrete set of adsorption sites separated by the Ag(111) nearest neighbor distance, 0.289 nm. Because rotation only occurred about an end atom, both rotation and lengthwise hopping displace the center of mass by one nearest neighbor spacing.

The low time resolution of the STM prevents direct knowledge of the intermediate steps in trimer chain diffusion, but important details of the intermediate steps can be inferred from the experimentally observed characteristics of lengthwise translation and end-atom rotation. The fact that rotation and lengthwise hopping occur at the same rate suggests that they share the same rate-limiting step. Moreover, the rotation direction depends on both the chain orientation and on which end of the chain moves. This dependence is illustrated in the models below the images in Fig. 3. Below (a), for example, two rotations are allowed. The other two rotations in the upward directions were not allowed. The key to such motion must be in the intermediate steps because the disallowed rotations would result in final states that are equivalent to those resulting from the allowed rotations. The solid circles indicate the initial atom locations, the open circles the final locations, and the arrows the directions of rotation.

For larger islands of Cu on Ag(111), diffusion occurred through the nucleation of misfit dislocations that shifted a portion of the atoms into hcp sites and shortened Cu-Cu bonds, reducing strain. Applying this rule to trimer chains results in exactly the rotation directions observed experimentally, as rationalized in Fig. 4, which illustrates possible pathways for lengthwise hopping (a)–(d) and end rotation (a), (e), and

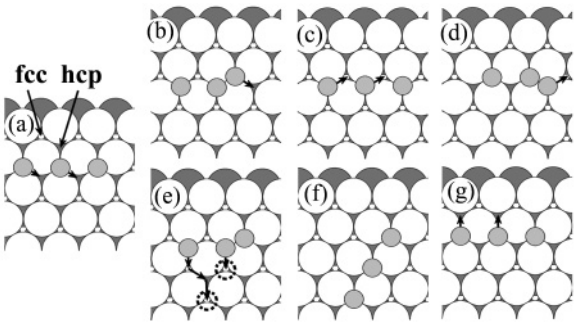

FIG. 4. Models showing displacements that could lead to the hopping (a)–(d) and rotation (a), (e), and (f) observed experimentally. With this model, rotation and hopping share a step (b) and (e) involving hcp sites. We argue that the lattice mismatch favors transitions from fcc-hcp that shorten Cu-Cu bonds, leading to the observed correlation between rotation direction and orientation. Rotation in the opposite direction is not allowed because this would involve fcc-hcp transitions that stretch Cu-Cu bonds (g).

(f) that share a step involving hcp sites that shorten Cu-Cu bonds. In this model, both hopping and rotation commence when two atoms shift into hcp sites, shown in the equivalent transitions of (a)–(b) and (a)–(e). For lengthwise hopping, this state is followed by one in which the third atom moves into an hcp site (b), and the hop of one nearest neighbor distance is completed by a similar piecewise motion of the trimer from hcp to fcc sites (c), (d). For rotation to occur, instead of the third atom moving into hcp stacking, the two atoms in hcp sites move further, as shown in (e). In this model, rotation only occurs in certain directions because rotation in the other directions would require the use of hcp sites that stretch the already strained Cu-Cu bonds, as illustrated in Fig. 4(g). The sequences shown in Fig. 4 cannot be verified experimentally, as intermediate diffusion steps are not observed, but they satisfy the requirement that an intermediate step involves hcp sites to shorten Cu-Cu bonds, and this is the only explanation for the observed rotation directions. Furthermore, motion occurs in a piecewise fashion, as concerted hopping and rotation would show no preference for certain hopping and rotation directions.

An individual linear trimer was tracked between 8.34 and 9.34 K, and Fig. 5 summarizes the temperature dependence of its lengthwise hop and rotation rates. The error bars represent the standard errors of the mean hop rates, and the numbers beside each point indicate the number of events observed. Both hopping (blue squares) and rotation (red triangles) occurred with nearly equal probability at each temperature investigated, and thus, when treated separately, the measured barriers and prefactors are within a standard error of each other: $\nu_o^h = 2.1 \times 10^{4\pm0.5}$ s^{-1}, $E_a^h = 12.7 \pm 1$ meV; $\nu_o^r = 3.0 \times 10^{5\pm0.8}$ s^{-1}, $E_a^r = 14.8 \pm 1.5$ meV. Because both rotation and lengthwise hopping resulted in displacement of the trimer center of mass by 0.289 nm, the overall diffusion rate (black circles) includes both hopping and rotation events with $\nu_o^d = 1.3 \times 10^{5\pm0.4}$ s^{-1} and $E_a^d = 13.6 \pm 0.7$ meV. The barriers, prefactors, and related uncertainties were determined using a weighted least-squares fit, where the weighting factors and uncertainties were derived from the standard deviation

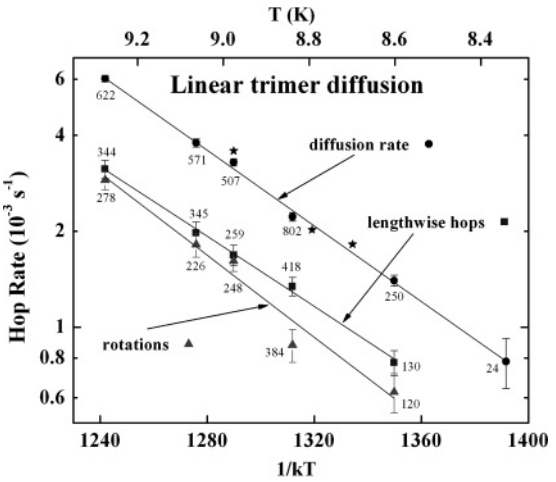

FIG. 5. Arrhenius plot of the temperature dependence of the rates of lengthwise hopping (blue squares), rotation (red triangles), and the combined diffusion rate (black circles). Hopping ($\nu_o^h = 2.1 \times 10^{4\pm0.5}$ s^{-1}, $E_a^h = 12.7 \pm 1$ meV) and rotation ($\nu_o^r = 3.0 \times 10^{5\pm0.8}$ s^{-1}, $E_a^r = 14.8 \pm 1.5$ meV) occurred with statistically indistinguishable rates, leading to the same net displacement of one nearest neighbor distance and the net diffusion rates indicated by the black circles ($\nu_o^d = 1.3 \times 10^{5\pm0.4}$ s^{-1}, $E_a^d = 13.6 \pm 0.7$ meV). The stars indicate diffusion rates measured for a second trimer chain that was constructed, indicating the reproducibility of the results.

of the measured time between hops and the number of hops observed.[39] Surprisingly, the diffusion barrier for linear trimers is only ∼1/5 of that for a Cu adatom on Ag(111), 65 meV. The prefactors reported for linear trimer diffusion are surprisingly low compared to the $\nu_o^d \sim 10^{12}$ s^{-1} expected for thermally activated diffusion. Although efforts were made to minimize the experimental errors in the diffusion parameters, the narrow temperature range accessible in the experiment makes it difficult to rule out all experimental uncertainty, and at present, there is no physical explanation for this low prefactor.

The finite scan rate of the STM limits the temperature window where hop rates can be measured directly. For these temperature-dependent measurements, the time interval between frames was ∼100 s. At 9.3 K, the highest temperature plotted in Fig. 5, the mean hop rate is ∼60% of the frame rate, giving a probability of ∼0.6 that a hop will occur within the time interval between images. Assuming a Poisson distribution for the number of hops between frames, one expects zero hops to occur for ∼55% of time intervals, a single hop to occur for ∼33% of time intervals, and two hops to occur for ∼10% of time intervals. This is in reasonable agreement with our observations of zero hops for ∼50%, one hop for ∼33%, and two hops for ∼8.5% of time intervals at 9.3 K, ensuring that hops could be counted accurately within the experimental temperature range. Furthermore, to test how well the fit could predict diffusion rates at higher temperatures, we measured the mean-squared displacement at 12 K, a temperature where multiple hops occurred between images, and the diffusion rate fell within a standard error of the extrapolated fit. Besides verifying that the parameters measured at 8–9 K made reasonable predictions, the measurements of mean squared displacements at elevated temperatures indicate that the tip had

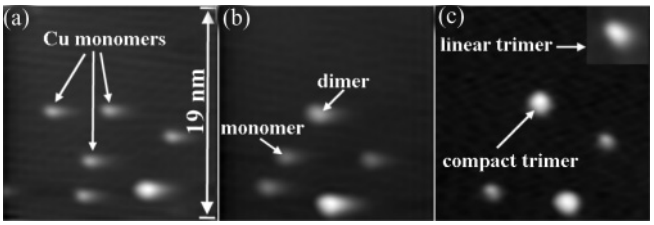

FIG. 6. Images showing the construction of a compact trimer at 5 K. Between frames (a) and (b), a dimer was formed by moving the left-most atom into the center atom. Between frames (b) and (c), a compact trimer was formed by moving the final atom into the dimer. The inset shows a linear trimer, allowing for comparison.

no significant influence on the measurements. Finally, to check the reproducibility of our results, we constructed a second linear trimer. It displayed the same rotation and lengthwise hopping and the same temperature dependence of the diffusion rate, as shown by the stars in Fig. 5.

A compact triangular trimer was also constructed at 5 K, as shown in Fig. 6. Three monomers are visible in (a), a dimer is formed in (b), and a compact trimer in (c). The inset in (c) is an image of a linear trimer for a comparison. Temperature-dependent measurements to 15 K showed that the compact trimer was immobile, as expected from the measurements at 24 K. No transition to the linear form was observed. Measurements with the linear trimers likewise showed no transitions to the compact structure. We conclude that hopping and rotation at 8–9 K do not involve interconversion between linear and compact forms, in agreement with our model.

We have shown that the diffusion barrier of a linear trimer is low enough to account for the displacements observed upon trimer nucleation at 24 K. Because every trimer nucleation event resulted in rapid relocation, this implies that the kinetically preferred pathway to the compact trimer involves the linear trimer. Besides translating, Cu dimers on Ag(111) undergo rotation among the three equivalent fcc sites surrounding a surface atom, resulting in three different orientations along the close-packed ⟨110⟩ directions. While the barrier for dimer diffusion is higher than that for atom diffusion, the barrier for dimer rotation is lower than that for atom diffusion. Morgenstern *et al.*[34,40] showed that surface-mediated adatom-dimer interactions perturb dimer rotation. With adatom-dimer separations of ∼1–2 nm (4–8 lattice spacings), one dimer orientation was favored over the other two. From the data presented in Ref. 34, and especially the supporting STM movies of Ref. 40, the preferred orientation is one that presents the end of a dimer, rather than the side, toward the third atom. The relatively low barrier for dimer rotation compared to atom diffusion would allow the dimer to rotate to the favored orientation upon the approach of a third atom. Thus, these surface-mediated atom-dimer interactions are likely the cause for the very strong bias in favor of linear trimer formation as a precursor to the thermodynamically favored compact trimer.

V. CONCLUSION

The types of motion reported here for trimers are very different from those reported in either experimental or theoretical studies of homoepitaxial fcc(111) trimers. For Ir_3 on Ir(111), both linear and triangular forms were observed, rotation required interconversion between the two forms, and translation was roughly four times more probable than rotation. Further, the mechanisms for Ir_3 do not limit center-of-mass displacements to one nearest neighbor distance, as we observe for Cu_3, but allow shorter displacements as well.[22] Molecular dynamics simulations of Al_3 on Al(111) show that trimer diffusion is similar to Ir_3, with interconversion between triangular and linear forms having barriers similar to those for translation.[41] Molecular dynamics simulations of Cu_3 on Cu(111) show that diffusion occurs through concerted gliding and rotation of the triangular form because this has a much smaller barrier than interconversion to the linear form.[42]

In contrast, our results show that linear trimer chains on Ag(111) diffuse through lengthwise translation and end-atom rotation, which occur with equal probability, with no conversion to the compact form. Compact trimers are stable and immobile up to at least 24 K, indicating high barriers for translation and conversion to the linear form. The extremely low diffusion barrier for the linear trimer, combined with the preference for this structure during nucleation, make the trimer an extremely important contributor to mass transport for Cu on Ag(111). The effects of lattice mismatch are manifest in the observed directions of hopping and rotation that require intermediate steps involving trimers of mixed fcc-hcp character that shorten Cu-Cu bonds to relieve strain, in a one-dimensional analog of the misfit-dislocation mechanism responsible for the low diffusion barriers of larger Cu clusters on Ag(111).[25,26] Because the novel diffusion phenomena for both small and large clusters of Cu on Ag(111) result from lattice mismatch, it is likely that similar behavior will occur in other heteroepitaxial systems.

ACKNOWLEDGMENTS

The authors thank H. H. Wu, D. R. Trinkle, R. E. Butera, G. Ehrlich, J. Lyding, and P. Swaminathan for fruitful discussions. This paper was supported by NSF DMR 0703995.

*jhweaver@illinois.edu

[1] G. Ehrlich, Surf. Sci. **246**, 1 (1991).
[2] T. T. Tsong, Rep. Prog. Phys. **51**, 759 (1988).
[3] A. G. Naumovets and Z. Y. Zhang, Surf. Sci. **500**, 414 (2002).
[4] A. G. Naumovets, Physica A **357**, 189 (2005).
[5] J. Venables, Philos. Mag. **27**, 697 (1973).
[6] J. Villain, A. Pimpinelli, L. Tang, and D. Wolf, J. Phys. (France) I **2**, 2107 (1992).
[7] M. C. Bartelt, S. Günther, E. Kopatzki, R. J. Behm, and J. W. Evans, Phys. Rev. B **53**, 4099 (1996).

[8]G. Rosenfeld, A. F. Becker, B. Poelsema, L. K. Verheij, and G. Comsa, Phys. Rev. Lett. **69**, 917 (1992).
[9]S. B. Lee, Phys. Rev. B **73**, 035437 (2006).
[10]K. Morgenstern, Phys. Status Solidi B **242**, 773 (2005).
[11]M. Giesen, Prog. Surf. Sci. **68**, 1 (2001).
[12]K. Morgenstern, E. Laegsgaard, and F. Besenbacher, Phys. Rev. Lett. **86**, 5739 (2001).
[13]K. Morgenstern, G. Rosenfeld, B. Poelsema, and G. Comsa, Phys. Rev. Lett. **74**, 2058 (1995).
[14]J. M. Wen, S. L. Chang, J. W. Burnett, J. W. Evans, and P. A. Thiel, Phys. Rev. Lett. **73**, 2591 (1994).
[15]D. C. Schlößer, K. Morgenstern, L. K. Verheij, G. Rosenfeld, F. Besenbacher, and G. Comsa, Surf. Sci. **465**, 19 (2000).
[16]K. Morgenstern, E. Lægsgaard, and F. Besenbacher, Phys. Rev. B **66**, 115408 (2002).
[17]S. V. Khare, N. C. Bartelt, and T. L. Einstein, Phys. Rev. Lett. **75**, 2148 (1995).
[18]S. V. Khare and T. L. Einstein, Phys. Rev. B **54**, 11752 (1996).
[19]G. L. Kellogg, Phys. Rev. Lett. **73**, 1833 (1994).
[20]J. C. Hamilton, M. S. Daw, and S. M. Foiles, Phys. Rev. Lett. **74**, 2760 (1995).
[21]J. C. Hamilton, Phys. Rev. Lett. **77**, 885 (1996).
[22]S. C. Wang and G. Ehrlich, Surf. Sci. **239**, 301 (1990).
[23]G. L. Kellogg, Appl. Surf. Sci. **67**, 134 (1992).
[24]S. C. Wang, U. Kurpick, and G. Ehrlich, Phys. Rev. Lett. **81**, 4923 (1998).
[25]H. H. Wu, A. W. Signor, and D. R. Trinkle, J. Appl. Phys. **108**, 023521 (2010).
[26]A. W. Signor, H. H. Wu, and D. R. Trinkle, Surf. Sci. Lett. **604**, L67 (2010).
[27]H. W. Fink and G. Ehrlich, Surf. Sci. **150**, 419 (1985).
[28]W. R. Graham and G. Ehrlich, Phys Rev. Lett. **31**, 1407 (1973).
[29]W. R. Graham and G. Ehrlich, J. Phys. F: Metal Phys. **4**, L212 (1974).
[30]K. Stolt, W. R. Graham, and G. Ehrlich, J. Chem. Phys. **65**, 3206 (1976).
[31]T. Sakata and S. Nakamura, Surf. Sci. **51**, 313 (1975).
[32]B. G. Briner, M. Doering, H. P. Rust, and A. M. Bradshaw, Science **278**, 257 (1997).
[33]L. Huang, S. J. Chey, and J. H. Weaver, Surf. Sci. **416**, L1101 (1998).
[34]K. Morgenstern, K. F. Braun, and K. H. Rieder, Phys. Rev. Lett. **93**, 056102 (2004).
[35]S. W. Hla, K. F. Braun, and K. H. Rieder, Phys. Rev. B **67**, 201402(R) (2003).
[36]J. Repp, G. Meyer, K. H. Rieder, and P. Hyldgaard, Phys. Rev. Lett. **91**, 206102 (2003).
[37]H. H. Wu and D. R. Trinkle, Comp. Mater. Sci. **47**, 577 (2009).
[38]J. C. Crocker and D. G. Grier, J. Colloid Interface Sci. **179**, 298 (1996).
[39]J. Cvetanovic and D. L. Singleton, J. Phys. Chem. **83**, 50 (1979).
[40]K. Morgenstern, New J. Phys. **7**, 139 (2005).
[41]C. M. Chang, C. M. Wei, and S. P. Chen, Surf. Sci. **465**, 65 (2000).
[42]A. Karim, A. N. Al-Rawi, A. Kara, T. S. Rahman, O. Trushin, and T. Ala-Nissila, Phys. Rev. B **73**, 165411 (2006).